Cathode materials evaluation in microbial fuel cells : a comparison of carbon, Mn2O3, Fe2O3 and platinum materials

Martin, Edith; Tartakovsky, Boris; Savadogo, Oumarou

Publisher's version / Version de l'éditeur:
https://doi.org/10.1016/j.electacta.2011.08.078
Electrochimica Acta, 58, pp. 58-66, 2011-09-22

Electrochimica Acta 58 (2011) 58–66

Contents lists available at SciVerse ScienceDirect

Electrochimica Acta

journal homepage: www.elsevier.com/locate/electacta

Cathode materials evaluation in microbial fuel cells: A comparison of carbon, Mn_2O_3, Fe_2O_3 and platinum materials

Edith Martin[a,b], Boris Tartakovsky[b], Oumarou Savadogo[a,*]

[a] Laboratory of Electrochemistry and Energetic Materials, École Polytechnique de Montréal, C.P.6079, Centre-Ville, Montreal, QC, Canada, H3 C 3A7
[b] Biotechnology Research Institute, NRC, 6100 Royalmount Ave, Montreal, QC, Canada, H4P 2A2

ARTICLE INFO

Article history:
Received 24 June 2011
Received in revised form 22 August 2011
Accepted 22 August 2011
Available online 22 September 2011

Keywords:
Microbial fuel cell
Cathode materials
Mn_2O_3
C
Fe_2O_3

ABSTRACT

In this work the oxygen reduction reaction (ORR) electro catalytic activity of Fe_2O_3 and Mn_2O_3 nanopowders, and carbon black powder was compared and evaluated against that of a Pt-cathode in an air-cathode microbial fuel cell (MFC) using several electrochemical techniques. The total resistance of the cathode electrode determined by impedance spectroscopy was 9.6, 7.8, 7.6 and 21.6 Ω for Pt, Mn_2O_3, Fe_2O_3 and C, respectively. Although the Mn_2O_3 cathode had the lowest resistance, the highest power output in polarization tests was observed for Pt, followed by Mn_2O_3, Fe_2O_3 and C. The corresponding volumetric power outputs were 90, 32, 15 and 8 W m^{-3}. The ORR onset potentials determined using cyclic voltammetry have shown values of 783, 844, 696 and 562 mV vs Ag/AgCl for Pt, Mn_2O_3, Fe_2O_3 and C, respectively. Therefore, Mn_2O_3 exhibited the best ORR potential, whereas Pt exhibited the best volumetric power output. The MFCs based on these cathodes showed a performance decline with time, most likely due to the loss of the catalyst, catalyst deactivation, or parasitic reactions. The MFC based on carbon cathode showed the most stable behavior. In all tests, biofilms were, of course, formed at the various cathodes, but a microbially catalyzed ORR (biocathode) or a biofilm catalytically active for the ORR was not observed. The Mn_2O_3 electrode appeared to be the most promising non-noble electro catalyst cathode; however its high overpotential (activation loss) should be improved in order to increase significantly the power generation.

1. Introduction

Microbial fuel cells provide an alternative method for simultaneous energy production and wastewater treatment. In a MFC consumption of organic compounds by microorganisms at the anode is accompanied by electron transfer to the anode and proton release. The protons flow through the electrolyte and the electrons flow through the external circuit to reach the cathode, where they are used along with electrons to accomplish oxygen reduction to water [1,2].

The oxygen reduction reaction (ORR) is an energetically costly reaction because of a high overpotential barrier when performed on carbon or graphite electrodes, implying the need for catalysts like platinum (Pt). In a MFC, Pt can lose a lot of its activity due to side reactions and other losses [3–8]. Several alternatives have been proposed to replace Pt: manganese oxides [9,10], polypyrrole (Ppy) [11], iron phthalocyanine (FePc) [12,13], cobalt and iron–copper phthalocyanine (CoPc and FeCuPc) [13], cobalt tetramethoxyphenylporphyrin (CoTMPP) [12,13], iron–cobalt tetramethoxyphenylporphyrin (FeCoTMPP) [13], Fe^{3+} cathode made with ferric sulfate [14], high surface area graphite-granules cathodes [8], and activated carbon [15–17]. Although manganese oxides, Ppy, FePc and CoTMPP show slightly less power generation than Pt, the low cost of these materials makes them a good replacement of Pt since these materials are less expensive. Some carbon/graphite electrodes also exhibit a good performance as cathode materials, which also make them suitable alternatives as they are inexpensive in comparison to other noble and non-noble materials.

Various cathode-oxidizing microorganisms are known to be capable of electron transfer from cathodes to either nitrate (denitrification) [18,19] or chromium (Cr^{4+}) [20,21]. Oxygen and protons are other potential electron acceptors and a wide variety of microorganisms have demonstrated their ability to use it [22]. However the effect of microorganisms on the oxygen reduction reaction (ORR) requires further clarification [23], although cytochromes, hydrogenase enzymes and mediators are assumed to participate in this reaction [24]. Cathodic biofilms were observed to catalyze the ORR [25]. Mn^{4+} and Fe^{3+} reduction is an important part of biocathodic activity [2,23]. Mn^{4+} reduction and Mn^{2+} oxidation is accomplished through several steps. The first step is the abiotic MnO_2 reduction to MnOOH by accepting one electron followed by

* Corresponding author. Tel.: +1 514 340 4725; fax: +1 514 340 4468.
E-mail address: osavadogo@polymtl.ca (O. Savadogo).

0013-4686/$ – see front matter © 2011 Elsevier Ltd. All rights reserved.
doi:10.1016/j.electacta.2011.08.078

the reduction of MnOOH to Mn^{2+} in solution by accepting a second electron. Mn^{2+} is then oxidized into MnO_2 by microorganisms that release two electrons to oxygen. Fe^{3+} reduction and Fe^{2+} oxidation is thought to work in a similar way as biological manganese transformation [20,23]. Mn^{2+} and Fe^{2+} oxidation is a rate-limiting process [26,27], however it could be accelerated due to microbial activity. Also, the materials used in this case may exhibit oxygen reduction to produce water using reactions similar to those with Pt catalyst [8,28]. This work is aimed at studying cathode materials (e.g. C, Mn_2O_3 and Fe_2O_3) suitable for MFC applications.

2. Experimental

2.1. Cathode preparation

Catalysts based on Pt, Mn_2O_3 and Fe_2O_3 were supported using carbon powder. Pt nanoparticles supported on carbon (EC-20-PTC) were purchased from ElectroChem, Inc., Woburn, MA, USA. Mn_2O_3 and Fe_2O_3 nanopowders with purity of 98.5 and >98% respectively were obtained from Nanostructured & Amorphous Materials, Inc., Houston, TX, USA and the Vulcan XC-72 carbon black powder was from Cabot Corporation, Boston, MA, USA. The Mn_2O_3 and Fe_2O_3 structures have been confirmed by X-ray diffraction (XRD) and thermogravimetric (TGA) analyses. The carbon-supported Pt catalyst had a nominal Pt loading of 20 wt%. Manganese and iron oxide nanopowders had respective average particles sizes of 30–60 and 20–50 nm and were both separately mixed with Vulcan powder to obtain an individual ratio of 20 wt% Mn_2O_3 and Fe_2O_3. The catalyst inks were prepared from Pt/C, pure Vulcan carbon powder, Mn_2O_3/C or Fe_2O_3/C powders and mixed with a Nafion® NR 005 solution (DuPont, Wilmington, DE, USA) to obtain loadings of 1 mg cm^{-2} with a catalyst: Nafion (dry weight) ratio of 65:35 wt%. Mixtures were sonicated (B5500-A-MTH, VWR, West Chester, PA, USA) for 1 h prior to their brush painting on 11 cm × 6 cm, 175 μm-thick carbon fiber papers treated with a PTFE hydrophobic coating (AvCarb™ P50T, Fuel Cell Store, San Diego, CA, USA). Cathodes were then air dried. At least 2 samples of 1 cm^2 were also made for each catalyst type in order to make half-cell electrochemical experiments.

2.2. MFC design and operation

A schematic diagram of the MFCs used for cathode testing is shown in Fig. 1. The anodes were made of 5 cm × 10 cm, 5 mm-thick carbon felt (Speer Canada, Kitchener, ON, Canada). The electrodes were separated with J-cloth® providing a spacing of approximately 1 mm. The anode and cathode were connected through an external load (R_{ext}). A data acquisition card (LabJack U12, LabJack Corporation, Colorado, USA) was used to record MFC voltage. More details of MFC design and operation can be found elsewhere [29].

The MFCs were operated at room temperature in a continuous flow mode with a hydraulic retention time of 12 h. Liquid mixing was accomplished by a peristaltic pump in an external recirculation line. Sodium acetate and nutrients were combined in a single concentrated solution fed at a rate of 5 mL d^{-1} by a syringe pump (model NE-1000, New Era Pump Systems, Inc., Wantagh, NY, USA). 1 mL of microelements stock solution was added to each liter of dilution water provided at a rate of 100 mL d^{-1} with a peristaltic pump.

Four membraneless air-cathode MFCs with a mature anodic biofilm were used. MFCs were started up with commercial gas diffusion cathodes with a Pt loading of 0.5 mg cm^{-2} (E-TEK Division, PEMEAS Fuel Cell Technologies, Somerset, NJ, USA). Once the maximum power generation at an optimal external loading was reached, E-TEK cathodes were replaced with laboratory-made cathodes and

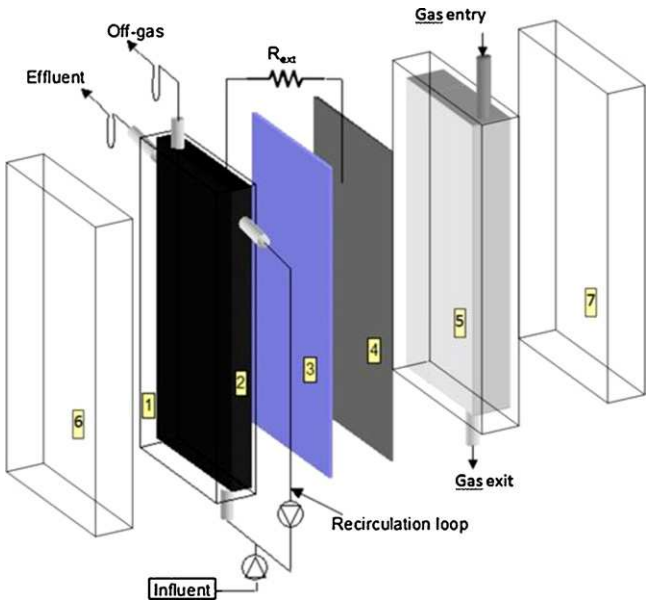

Fig. 1. MFC setup diagram showing external resistance (R_{ext}), recirculation loop, influent and gas entries, effluent and gas exits, anodic windowed plate (1), anode (2), J-cloth® (3), cathode (4), cathodic windowed plate (5) and closing plates (6 and 7).

the MFCs were operated for two weeks to one month. Testing has been done in triplicate for each material type. In some tests the cathodic chamber was saturated with pure nitrogen for 24 h and then with pure oxygen for 48 h after MFC operation under the atmosphere of air.

2.3. Inoculum and media composition

The MFCs were inoculated with the effluent of another working MFC previously inoculated with homogenized anaerobic mesophilic sludge (VSS = 50 g L^{-1}, A. Lassonde Inc., Rougemont, Quebec, Canada). The stock solution of microelements contained (g L^{-1}): $FeCl_2{\cdot}4H_2O$ (2), H_3BO_3 (0.05), $ZnCl_2$ (0.05), $CuCl_2$ (0.03), $MnCl_2{\cdot}4H_2O$ (0.5), $(NH_4)_6Mo_7O_{24}{\cdot}4H_2O$ (0.05), $AlCl_3$ (0.05), $CoCl_2{\cdot}6H_2O$ (0.05), $NiCl_2$ (0.05), EDTA (0.5) and HCl (1 μL). The feed stock solution contained (g L^{-1}): yeast extract (0.83), NH_4Cl (18.68), KCl (148.09), K_2HPO_4 (64.04), KH_2PO_4 (40.69), and anhydrous sodium acetate (54.67).

2.4. Electrochemical measurements

The electrochemical impedance spectroscopy (EIS) tests were performed with a frequency response analyzer (FRA) (Model 1260A, Solartron Analytical, Hampshire, UK) connected to a potentiostat (Solartron 1470, Solartron Analytical, Hampshire, UK). ZPlot and ZView software (Solartron Analytical, Hampshire, UK) were used as potentiostat and FRA controller and for data analysis respectively. EIS experiments were carried out in a three-electrode mode, the cathode as the working electrode, the anode as the counter electrode and a 1 M Ag/AgCl electrode (222 mV vs SHE) as the reference. The measurements were performed at cathode working potentials while MFCs were operated at a constant R_{ext} in order to study the cathode behavior during MFC operation. EIS tests were performed at an AC signal of 5 mV of amplitude, at 37 logarithmic frequency steps between 100 kHz and 5 mHz (duration of approximately 30 min).

The acquired EIS spectra of cathodes showed a three-time-constant model (three semi-circles). The low-frequency semi-circle is attributed to a cathodic charge transfer (ct) while the

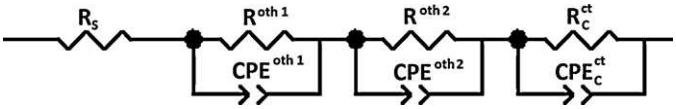

Fig. 2. Three time constants equivalent circuit for EIS data fitting.

high-frequency semi-circles may be attributed to other various causes related to the electrolyte composition, or diffusion of the oxygen or protons in the electrolyte, or diffusion through a biofilm (oth 1 and 2). Hence, the electrical equivalent circuit presented in Fig. 2 was used to fit the data. Here, R_S is the solution resistance, R^{oth} is the resistances of further redox processes and CPE^{oth} is the constant phase element, R_C^{ct} is the cathodic charge transfer resistance for oxygen reduction, and CPE^{ct} is the constant phase element related to charge transfer. Constant phase elements (CPE) are used instead of standard capacitances in the modeling because of the inhomogeneous conditions (roughness, porosity, distribution of reaction sites) [30]. Fitting the semi-circles with a CPE allows to account for the process capacitance and for the influence of diffusion and electrode structure.

Cyclic voltammetry (CV) was performed using a potentiostat (Solartron 1470, Solartron Analytical, Hampshire, UK) in a three-electrode mode. CorrWare and CorrView software (Solartron Analytical, Hampshire, UK) were used for potentiostat control and data analysis, respectively. Cathode and anode were used as working and counter electrodes, respectively. The reference electrode was a 1 M Ag/AgCl electrode. Three cycles were carried out at scan rates of 5 mV s^{-1} at potential values varying between −0.4 and 1 V vs Ag/AgCl, depending on cathode atmosphere and cathode materials. Tafel slopes (b) were handled as being part of the overpotential (η) as shown in the following equation:

$$\eta = E_{OCP} - E_{work} = b \ln \frac{i}{i_0}$$

where E_{OCP} and E_{work} are cathode potentials at the open circuit and working voltages, respectively, i is the current produced at the working potential and i_0 is the limiting current.

Cyclic voltammetry was also performed in the half-cells under N_2 and O_2 atmospheres with non-colonized 1 cm^2 samples and with colonized 1 cm^2 samples taken from cathodes used during MFC operation. For the half-cell experiments, the samples were immersed in solutions similar to those used for MFC operation (acetate and dilution water) and were used as working electrodes, while a pure platinum grid was used as a counter electrode, the reference was a saturated calomel electrode (SCE, 241 mV vs SHE). The tests were performed at voltages between −1 and 1 V at a scan rate of 10 mV s^{-1} for three cycles.

Linear polarization and power curves were acquired with a potentiostat (Solartron 1470, Solartron Analytical, Hampshire, UK) controlling the cell voltage (E_{MFC}) while measuring the generated current (I), from open circuit voltage (OCV) to short circuit at a scan rate of 0.5 mV s^{-1}. The anode was employed as the working electrode while the cathode was used as the counter and reference electrode. Anode and cathode potentials were measured against 1 M Ag/AgCl references via a data acquisition card (LabJack U12, LabJack Corporation, Colorado, USA).

Power (P) was calculated as $P = E_{MFC} \times I$. MFC voltage and power were plotted against current, to evaluate the MFC internal resistance (R_{int}) as the slope of the linear part of the polarization curve (E_{MFC} vs I), and the maximum power output (P_{max}) in the power curve. Anode and cathode potentials were also plotted against the current, which allowed for estimating anode and cathode resistances (R_A and R_C respectively) from the linear part of corresponding curves.

The cyclic voltammetry and polarization tests were periodically performed starting from the first day of cathode installation in MFCs to evaluate the cathode performance. Except for the first day of each test, the order of the electrochemical tests was as follows: EIS measurements at a working cathodic potential (V_{app}) was followed by voltage monitoring at open-circuit for 1 h before carrying out cyclic voltammetry. The MFCs were then left in open-circuit again for 1 h before performing the linear polarization test. The half-cell testing sequence consisted of: (1) solution flushing with N_2 for 1 h at an open circuit potential (OCP); (2) performing 100 activation cycles at a scan rate of 100 mV s^{-1} prior to carrying out cyclic voltammetry tests; and (3) O_2 flushing for 2 h at OCP before repeating the CV tests.

2.5. Analytical methods and calculations

The acetic acid concentration in the effluent was measured by gas chromatography (GC) using an Agilent 6890 (Wilmington, DE) with a detection limit of 0.2 mg L^{-1}. Manganese and iron concentrations have been determined in MFC effluent and in half-cell test solutions by atomic absorption spectroscopy (Analyst 200, Perkin-Elmer, Waltham, MA, USA).

The apparent Coulombic efficiency (CE_A) calculation can be seen in a previous work [29]. The degradation efficiency was evaluated by calculating the chemical oxygen demand (COD) removal with the following formula:

$$\frac{M_{in} - M_{out}}{M_{in}}(\%) = \frac{(F_{in} \cdot C_{stock}) - (F_{out} \cdot C_{out})}{(F_{in} \cdot C_{stock})} \times 100\%$$

where F_{in} and F_{out} are respectively the stock solution and the effluent flow rates (L s^{-1}), and C_{stock} and C_{out} are the acetate concentration in stock solution and acetate concentration in effluent, respectively (g L^{-1}).

The relative performance of cathodes under ambient air and saturated O_2 atmospheres $P_{cathode}^{atmosphere}$ was evaluated by measuring maximum power generation in air and pure oxygen atmosphere and comparing these values with platinum performance in air (P_{Pt}^{air}) one day after cathode installation. The following equation was used:

$$\text{Efficiency}(\%) = \frac{P_{cathode}^{atmosphere}}{P_{Pt}^{air}} \times 100$$

This is not an appropriate definition of the efficiency. But it is a useful parameter which helps to compare the relative performance of each type of cathode (carbon, Fe_2O_3, Mn_2O_3 and Pt) to those of platinum for this reaction. Accordingly, we used the ratio of the power generated by each cathode on the power generated by the Pt electrode in air. The values of this relative performance are indicated in the last column of Table 1.

3. Results

The data in Table 1 show the parameters obtained from electrochemical tests (EIS, CV and polarization tests) for all tested cathode materials and under different cathode atmospheres (air and O_2). Cathode performance is reported after approximately 1 and 10 days of electrode installation in the MFC. After installing new C, Fe_2O_3, Mn_2O_3 and Pt cathodes, a slight decrease in overall MFC performance was observed (P_{max} and ORR decrease, and R_{int}, R_C augmentation). Since MFCs under nitrogen cathodic atmosphere showed negligible current (parasitic current), these results are not shown. When results of EIS measurements were used to estimate charge transfer (R_C^{ct}) and total (R_C^{total}) resistances of different cathode materials, it was noted that after 10 days of cathode operation carbon exhibits the highest resistance (21.6 Ω), while

Table 1
Electrochemical parameters of cathode materials under atmospheres of air and O_2.

Materials	Atmosphere[a]	EIS		CV		Polarization		
		R_C^{ct} (Ω)	R_C^{total} (Ω)	ORR onset (mV)[c]	P_{max} (W m^{-3})	R_{int} (Ω)	R_C (Ω)	Relative performance or efficiency (%)
C	Air (1 day)	19.8 ± 2.8	22.7 ± 2.1	640.4 ± 37.3	9.8 ± 0.2	43.7 ± 8.4	21.3 ± 4.5	10.2
	Air (10 days)	18.4 ± 0.3	21.6 ± 0.3	561.7 ± 9.0	8.1 ± 0.9	45.1 ± 8.1	18.9 ± 3.3	8.4
	O_2 (13 days)	18.1 ± 2.4	21.4 ± 2.5	595.9 ± 11.2	12.7 ± 0.9	58.1 ± 13.3	25.4 ± 5.5	13.2
Fe_2O_3	Air (1 day)	5.3 ± 0.0	7.2 ± 0.4	720.0 ± 5.3	18.9 ± 2.8	16.8 ± 0.9	6.6 ± 0.2	19.6
	Air (10 days)	5.7 ± 0.7	7.6 ± 1.0	695.8 ± 5.2	15.4 ± 4.7	21.2 ± 6.6	9.7 ± 4.6	16.0
	O_2	4.1 ± 0.4	5.7 ± 0.4	724.6 ± 0.9	24.9 ± 5.4	17.1 ± 2.0	6.5 ± 0.0	25.9
Mn_2O_3	Air (1 day)	5.6[b]	7.7[b]	817.4 ± 4.1	44.4 ± 0.1	7.2 ± 0.8	3.3 ± 0.8	46.2
	Air (10 days)	5.8 ± 0.4	7.8 ± 0.4	844.1 ± 3.1	31.7 ± 1.6	8.7 ± 0.3	4.4 ± 0.5	33.0
	O_2	3.6 ± 0.4	5.9 ± 0.5	855.2 ± 3.3	45.1 ± 3.3	8.6 ± 0.5	4.0 ± 0.5	46.9
Pt	Air (1 day)	8.3[b]	9.7[b]	797.6[b]	96.2 ± 6.3	18.5 ± 1.1	10.4 ± 0.4	100
	Air (10 days)	7.9 ± 0.3	9.6 ± 0.5	782.8 ± 10.2	89.5 ± 3.2	18.4 ± 0.9	10.9 ± 0.4	93.0
	O_2	4.4 ± 0.5	5.8 ± 0.5	721.3[b]	83.2 ± 2.9	19.7 ± 2.3	9.9 ± 1.8	86.5

[a] Parameters determined after 1 and 10 days for air and 13 days for O_2 atmospheres.
[b] Average not available.
[c] Potential vs. Ag/AgCl.

other materials show lower resistances between 7.6 and 9.6 Ω. Pt has a higher resistance than the oxides tested. Also, impedance tests demonstrate the positive effect of O_2 on cathode resistance. When N_2 is introduced in the cathode chamber, the cathode resistance increases significantly. From Fig. 3, we note a solution resistance varying between 1.5 and 2 Ω (where EIS spectra intersect with the abscissa in a high-frequency region). Further side processes account for approximately 0.6 to 1 Ω in the total cathodic resistance. In the presence of air or oxygen, the relative performance of each type of cathode (carbon, Fe_2O_3, Mn_2O_3 and Pt) was determined (last column of Table 1) and we used the ratio of the power generated by each cathode on the power generated by the Pt electrode in air to characterise this parameter. The best relative performances are of course obtained for Pt. Mn_2O_3 based cathodes exhibit the second best performances in air or oxygen. When the testing time increases the relative performance decrease due to a decrease of the active sites related probably to the poisoning effect of the active sites.

Cyclic voltammetry tests (Fig. 4) demonstrate that the oxygen reduction reaction (ORR) takes place at different potentials depending on cathodic materials, time and atmosphere. MFC testing in air after 10 days of cathode operation indicate that the ORR onset occurs at the highest potential for Mn_2O_3 (844 mV vs Ag/AgCl), followed by Pt, Fe_2O_3 and C (783, 696 and 562 mV vs Ag/AgCl, respectively) (Table 1 and Fig. 4). Switching from an air to N_2 atmosphere decreases the ORR onset potential except in the case of Fe_2O_3, where it increases. An O_2 atmosphere increases the ORR potential for Mn_2O_3, Fe_2O_3 and C and decreases the potential for Pt when compared to air, but in all cases it increases ORR potentials when compared to N_2. With time, the ORR decreases for all cathode materials except Mn_2O_3 where it increases. N_2 results are not shown in Table 1.

The curves in Fig. 4 show a prolonged plateau in the forward scan (oxidation process) because it is probably due to the limiting factor of the adsorption of the oxidative species (oxygen for example) during the oxidation process when the potential increases to form oxides at higher potentials. The relative importance of the curves (in particular the hydrogen evolution peak) going presumably in the hydrogen region depends on the activity of the electrode for this reaction. More the hydrogen peak or the curves are going in the negative potential regions, less the electrode is theoretically active for the hydrogen evolution reaction.

Half-cell cyclic voltammetry (Table 2) analysis showed slightly different results as the ORR onset potential was also observed to take place at the highest potential for Mn_2O_3 (837 mV vs Ag/AgCl), but this was followed by Fe_2O_3 (832 mV vs Ag/AgCl) in an O_2 saturated solution. Carbon was observed to exhibit a higher ORR onset potential than Pt in half-cell tests (834 and 746 mV vs Ag/AgCl, respectively). Under a nitrogen atmosphere, manganese oxide still shows the highest onset potential. It is followed by C, Fe_2O_3 and finally Pt. Overall, N_2 decreased the onset potential only for Mn_2O_3 and Pt in half-cell tests.

As shown in Fig. 5 and Table 1, the polarization tests confirmed the poor performance of carbon cathodes for the oxygen reduction reaction since these cathodes exhibit the lowest power density (8 W m^{-3}) and the highest cell, anode and cathode resistances (45, 25 and 19 Ω respectively) after 10-days of testing in MFCs. On the

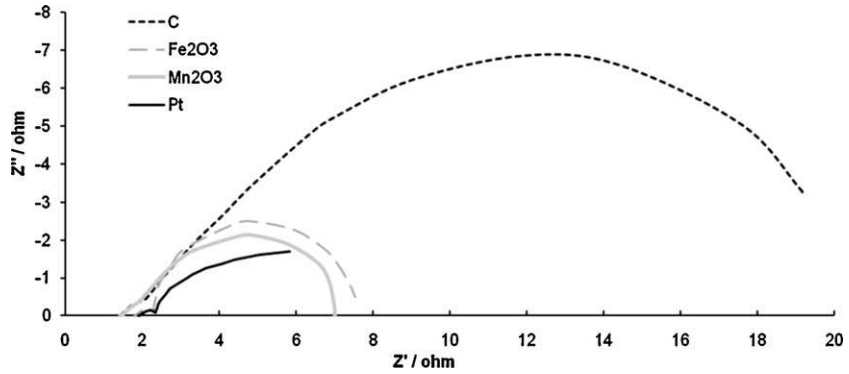

Fig. 3. EIS spectra of cathodes inserted in MFCs.

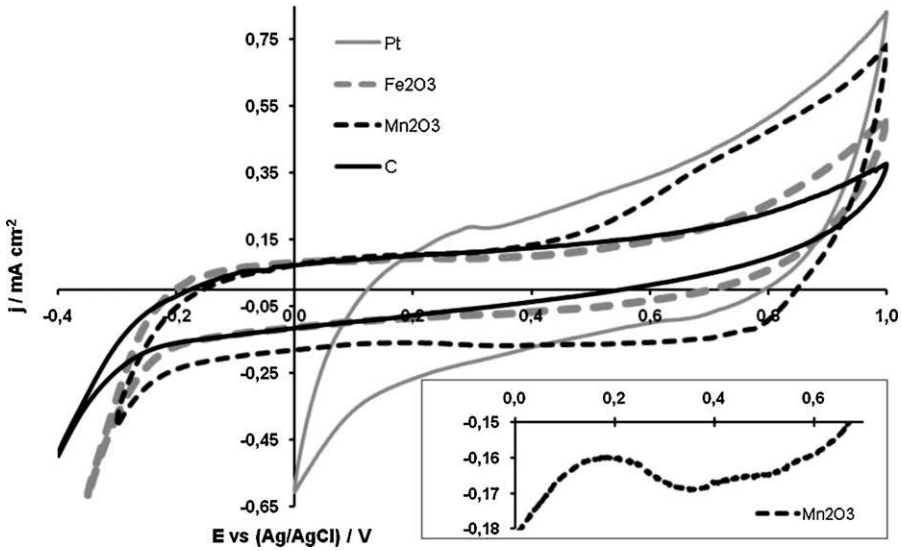

Fig. 4. Voltammograms of cathode materials at 5 mV s^{-1}, 10 days after insertion (inset: Mn_2O_3 reduction peak into Mn^{2+}). The organic load rate was 4 g L^{-1} d^{-1}. The MFCs were inoculated with the effluent of another working MFC previously inoculated with homogenized anaerobic mesophilic sludge (VSS = 50 g L^{-1}, A. Lassonde Inc., Rougemont, Quebec, Canada). The stock solution of microelements contained (g L^{-1}): $FeCl_2$ $4H_2O$ (2), H_3BO_3 (0.05), $ZnCl_2$ (0.05), $CuCl_2$ (0.03), $MnCl_2$ $4H_2O$ (0.5), $(NH_4)6Mo_7O_{24}$ $4H_2O$ (0.05), $AlCl_3$ (0.05), $CoCl_2$ 6H2O (0.05), $NiCl_2$ (0.05), EDTA (0.5) and HCl (1 μL). The feed stock solution contained (g L^{-1}): yeast extract (0.83), NH_4Cl (18.68), KCl (148.09), K_2HPO_4 (64.04), KH_2PO_4 (40.69), and anhydrous sodium acetate (54.67).

other hand, Mn_2O_3 displays the lowest resistances but does not show the highest power generation, which is obtained with Pt cathodes (32 W m^{-3} vs 90 W m^{-3}). Also, Pt and Fe_2O_3 give similar cell and electrode resistances, but their volumetric power output is significantly different. When the cathodic compartment is under an N_2 atmosphere, the MFCs show a negligible current production for all materials. In contrast, power generation increases in an O_2 atmosphere for C, Fe_2O_3 and Mn_2O_3 catalysts while the cathode resistances decrease for Fe_2O_3, Mn_2O_3 and Pt catalysts. A comparison of the polarization curves for different cathode atmospheres is shown in Fig. 6.

Overpotentials were evaluated for each cathode material after a 10-day cathode test in a MFC. Overpotentials of 179.0, 239.2, 400.6 and 284.0 mV were obtained for C, Fe_2O_3, Mn_2O_3 and Pt cathodes respectively. Hence, the Mn_2O_3 catalyst shows the highest potential loss between the cell open circuit and working voltages.

An evaluation of MFC efficiencies after the first day of MFC operation with C, Fe_2O_3 and Mn_2O_3 cathode catalysts showed efficiencies of 10.2%, 19.6% and 46.2%, respectively when compared to a Pt cathode in air at the same period (Table 1). After 10 days of MFC operation the efficiency declined to 17.3%, 18.5%, 28.6% and 7.0% for C, Fe_2O_3, Mn_2O_3 and Pt cathodes, respectively. Also, MFC operation under an O_2 atmosphere in the cathode chamber gave efficiencies of 13.2%, 25.9%, 46.9% and 86.5% for C, Fe_2O_3, Mn_2O_3 and Pt, respectively, in comparison to the highest power generated by Pt.

COD removal and Coulombic efficiency calculations agreed with the results of the polarization tests (Table 3). Pt cathodes demonstrate the highest efficiencies for acetate removal and utilization for electricity generation in an air atmosphere, followed by Mn_2O_3,

Table 2
ORR onset potentials of cathode materials under atmospheres of O_2 and N_2 in a half-cell.

Materials	Atmosphere	ORR onset (mV)[b]
C	N_2	834.3 ± 1.0
	O_2	817.1[a]
	O_2 with biofilm	646.3[a]
Fe_2O_3	N_2	832.3 ± 0.1
	O_2	821.5 ± 6.8
	O_2 with biofilm	765.5[a]
Mn_2O_3	N_2	836.7 ± 2.2
	O_2	850.7 ± 6.8
	O_2 with biofilm	696.4 ± 3.4
Pt	N_2	745.6 ± 13.5
	O_2	765.8 ± 2.7
	O_2 with biofilm	746.4 ± 36.9

[a] Average not available.
[b] Potential vs. Ag/AgCl.

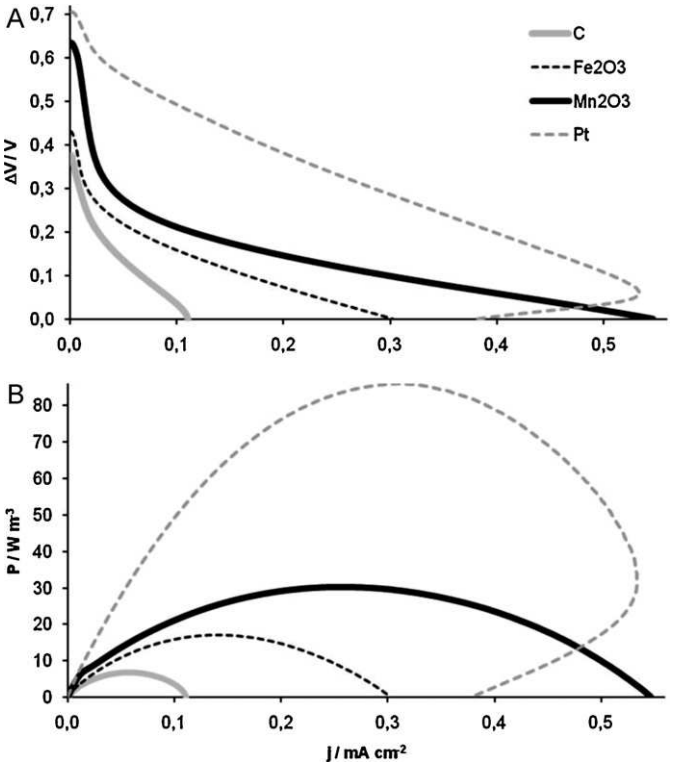

Fig. 5. Polarization (A) and power (B) curves of cathodic materials in air 10 days after insertion in MFCs.

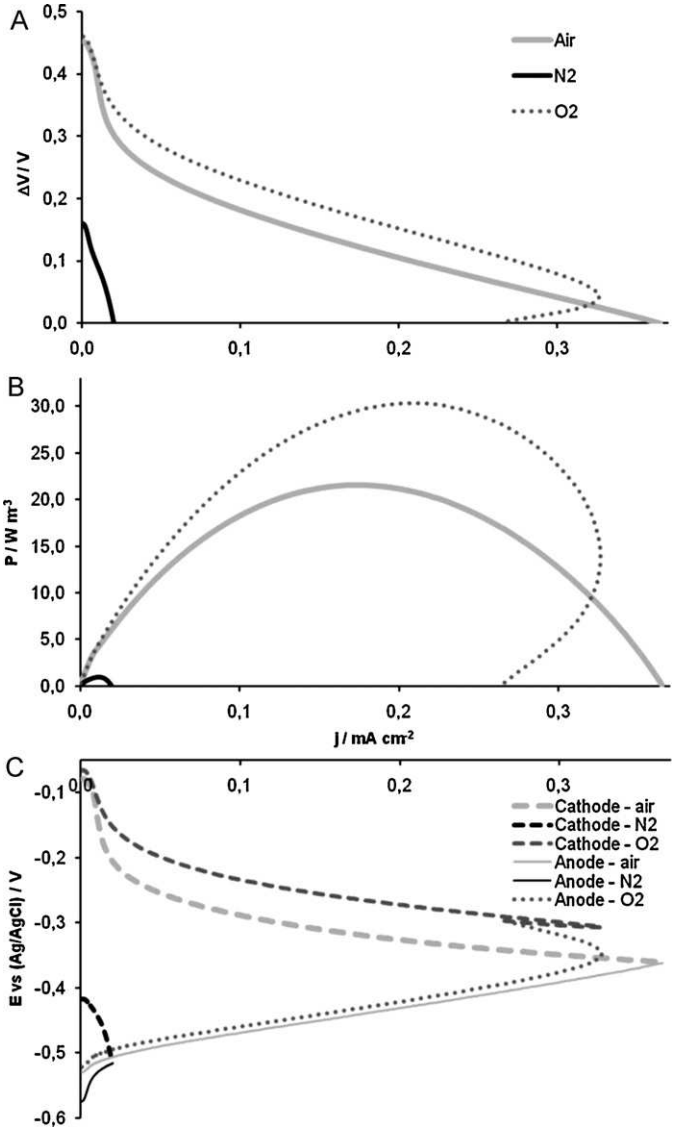

Fig. 6. Voltage vs current density polarization curves (A) and power vs current density (B) curves and electrodes potential (C) during polarization of Fe_2O_3 cathode in air, N_2 and O_2 atmospheres at a scan rate of 0.5 mV s^{-1}. The organic load rate was 4 g L^{-1} d^{-1}. The MFCs were inoculated with the effluent of another working MFC previously inoculated with homogenized anaerobic mesophilic sludge (VSS = 50 g L^{-1}, A. Lassonde Inc., Rougemont, Quebec, Canada). The stock solution of microelements contained (g L^{-1}): $FeCl_2$ $4H_2O$ (2), H_3BO_3 (0.05), $ZnCl_2$ (0.05), $CuCl_2$ (0.03), $MnCl_2$ $4H_2O$ (0.5), $(NH_4)6Mo_7O_{24}$ $4H_2O$ (0.05), $AlCl_3$ (0.05), $CoCl_2$ $6H_2O$ (0.05), $NiCl_2$ (0.05), EDTA (0.5) and HCl (1 μL). The feed stock solution contained (g L^{-1}): yeast extract (0.83), NH4Cl (18.68), KCl (148.09), K_2HPO_4 (64.04), KH_2PO_4 (40.69), and anhydrous sodium acetate (54.67).

Table 3
COD removal and coulombic efficiency (CE) of cathodic materials under atmospheres of air and O_2.

Materials	Atmosphere[a]	COD removal (%)	CE (%)
C	Air	64.5 ± 0.2	12.9 ± 0.4
	O_2	69.9 ± 5.5	15.0 ± 1.7
Fe_2O_3	Air	71.1 ± 9.1	24.2 ± 1.9
	O_2	73.9 ± 0.7	31.4 ± 3.1
Mn_2O_3	Air	86.5 ± 0.5	35.2 ± 3.7
	O_2	99.4[b]	42.6[b]
Pt	Air	85.3 ± 0.5	47.2 ± 2.7
	O_2	83.2 ± 8.1	45.3 ± 3.7

[a] Parameters determined after 10 days for air and 13 days for O_2 atmospheres.
[b] Average not available.

Table 4
Iron and manganese concentrations in MFC and half-cell solutions for C, Fe_2O_3 and Mn_2O_3 cathodes.

MFC	Mn (ppm)	Fe (ppm)
C	0.124	0.222
Fe_2O_3 (1 day)	0.115	0.176
Fe_2O_3 (9 days)	0.121	0.241
Mn_2O_3 (1 day)	0.696	0.202
Mn_2O_3 (8 days)	0.185	0.204
Half cell	Mn (ppm)	Fe (ppm)
C	0.187	0.305
Fe_2O_3	0.179	0.282
Mn_2O_3	0.361	0.379

Fe_2O_3 and C cathode materials. As expected, an N_2 atmosphere causes a significant decrease in COD removal and CE (data not shown). However, an oxygen atmosphere enhances COD removal and CE for C, Fe_2O_3 and Mn_2O_3 cathodes.

Iron and manganese ion concentrations in solution with C, Fe_2O_3 and Mn_2O_3 cathodes were evaluated in MFC and half-cell tests (Table 4). The ion concentration in the electrolytes with carbon cathodes was used as controls. Iron in all solutions stayed at a level close to the concentration measured in MFCs with C cathodes. However, manganese levels increased significantly with Mn_2O_3 cathodes both in half-cells and MFCs. Moreover, a higher manganese ion concentration was observed after one day of Mn_2O_3 cathode operation than after 8-day tests.

After 2–4 weeks, the cathodes were removed and an environmental scanning electron microscopy study was undertaken using cathode samples (images not shown). From these observations the biofilm thickness was estimated to be approximately 10–20 μm. All materials showed identical surface aspects, grown biofilms and microorganisms of similar shape.

3.1. Discussion

MFC operation with C, Fe_2O_3 and Mn_2O_3 cathode catalysts enables a comparison of their catalytic properties in a MFC as well as the suitability of these materials to stimulate biocathodic activity. Importantly, all MFC tests were started with Pt-containing cathodes. The cathodes to be tested were installed after observing a stable power output. Owing to well-colonized anodes, after the cathodes were replaced stable power outputs were observed within 1 h. Because of the very short time elapsed after cathode replacement, we related this power output to the electrochemical activity of the cathode. After the installation of new Fe_2O_3, Mn_2O_3 and Pt cathodes, a decrease in MFC performance was observed over a 10-day testing period (Table 1). This reduction was most likely caused by loss of catalyst in electrolyte and its deactivation (poisoning) with time by the electrolyte components [3,5,7], parasitic reactions caused partly by the biofilm formed on cathode or incomplete oxygen reduction (generation of OH^- or H_2O_2) [4,6,31]. Also, this reduction could be attributed to decreased current generation because the anode was frequently used in the electrochemical tests as a counter electrode (current reversal) which may have slightly damage the anode-reductive biofilm [32]. Performances of carbon cathodes were the most stable over the testing period since no catalyst can leach or be poisoned and the current generated by this material is not high enough to damage the anodic biofilm when the anode is used as a counter electrode.

The development of biocatalytic activity was anticipated at least on C cathodes [33–35], however their performance did not increase with time, which should happen with the growth of an active cathodic biofilm. Therefore, it was concluded that carbon only showed standard electrochemical behavior with a high cathodic

overpotential for ORR. Other tested materials worked as electrochemical catalysts since their performance declined significantly with time. These conclusions are supported by cyclic voltammograms (Fig. 4) showing that the oxidation branch of the ORR CV curves starts at 105, −235, −225 and −255 mV vs Ag/AgCl for Pt, Mn_2O_3, Fe_2O_3 and C, respectively. These values correspond to the cathodic working potentials measured during MFC operation, assuming that the oxygen reduction reaction takes place at the material surface in all cases. Moreover, a change in activation losses has not been observed during the testing period on each material, indicating that there might not have any increase of active bacteria population at the cathode and/or no improvement of the cathodic reaction. Although biofilm formation at the cathode surface was visually observed and confirmed by scanning microscopy, a significant increase in the cathodic activity was not observed with time. This suggests that biofilm formation alone at the cathode is not a sufficient condition for observing biocathodic activity, but that the proliferation of electrochemically active population is required.

EIS measurements (Table 1) showed that the resistances related to the electrolyte and secondary reactions accounted for a maximum of 3 Ω, which may be slightly influenced by a minor solution composition change and a reference electrode displacement between measurements. Thus approximately 10–25% of total cathodic resistance is a source of power loss related to solution resistance and other processes on cathode materials. From the shapes of the EIS spectra shown in Fig. 3, we can assume that the Pt-cathode behavior can be mostly attributed to a limited diffusion process since its charge transfer reaction is a more flattened semicircle than those of the other tested cathodes. This conclusion is supported by a CPE parameter fitting and by the decrease of the charge transfer resistance (R_C^{ct}) in the presence of the saturated O_2 atmosphere and the increase of the diffusion limitations that still appear on the EIS spectra.

The Mn_2O_3 cyclic voltammograms (Fig. 4 insert) show reduction peaks occurring at potentials between 0.25 and 0.55 V vs Ag/AgCl/V, which most likely corresponds to Mn^{2+} release into solution [23,27,36]. This reduction peak is more pronounced at the beginning of cathode operation and then it decreases considerably. These results are supported by atomic absorption analysis (Table 4), indicating a high manganese ion release in solution. This phenomenon was not observed for Fe_2O_3 or other materials. Since this reduction takes place at a potential much higher than the cathode working potential for Mn_2O_3, we believe that during normal MFC operation, a significant amount of Mn^{2+} ions would not be released, a release that would stimulate the development and the activity of an ORR active cathodic biofilm. However, a cathodic reaction improvement was not observed in our MFCs with high Mn^{2+} release during voltammetry, even in a MFC that was operated for more than three months (results not shown). The cathodic activity not improving over time is consistent with a previous study, where an improvement of biocathode power generation with manganese oxide deposition onto the cathode was not observed, although an increase of active cathodic biofilm formation was noticed [37].

From half-cell tests with 1 cm^2 non-colonized and colonized cathode samples, a negative effect of the biofilm on the ORR potentials was observed in all cases. The electrodes ORR onset potential decreased in the presence of bacteria. The ORR onset potentials also decreased over time (14 days to one month) in MFCs, confirming the negative impact of biofilm on ORR. The biofilm observed on the cathodes surface was expected to be ORR active. We may assume the negative effect of the biofilm formed on the cathode's catalyst (e.g. catalyst poisoning) or by parasitic activity. We did not observe a significant electrode resistance change during the early stages of biofilm growth (14 days to one month), despite observing a decreasing ORR onset potential and catalytic activity. This observation thus differs from the results obtained by Yang et al. [38], where electrode resistance was observed to be negatively affected by the cathodic biofilm.

In general, it is considered that a high OCV (open circuit voltage) is correlated to a good MFC performance. Platinum and Mn_2O_3 possess the two highest OCVs, 705 and 634 mV, respectively, as can be seen from Fig. 5. However, the power generated by Pt cathodes is almost 3-times higher than that generated by Mn_2O_3 and 5 and 11 times higher than the power generated by Fe_2O_3 and C cathodes respectively. The OCV is only partially related to the performance of the MFC. The activity of the oxide can also be related to the availability of the released metallic ions of the oxide, which may improve the ORR. In the case of Mn_2O_3, its high cathodic overpotential (400 mV) is most likely the cause of its lower than expected power generation. On the other hand, iron ions are highly insoluble at a pH higher than 2.5 [6,36] and Fe_2O_3 is a particularly stable oxide, which may explain its poor performance for ORR. It is well-known [6,8] that carbon electrodes exhibit a very poor ORR because of its inertia for this reaction, its elevated overpotential and low activity. This explains the EIS and polarization results in this work that demonstrate a higher total cathodic resistance for C cathodes when compared to other materials.

From Fig. 5A, we can note that the activation losses of Pt, Mn_2O_3, Fe_2O_3 and C cathodes decrease their MFC potential by approximately 100, 300, 125 and 150 mV respectively. By taking the slope of the first linear part of the polarization curves the activation losses of different materials can be compared. Pt, Mn_2O_3, Fe_2O_3 and C cathodes have respective slopes of 96, 271, 183 and 169 Ω. These results illustrate why Mn_2O_3 shows a high overpotential and low power output despite exhibiting a relatively high OCP. Platinum is the best catalyst among the four materials. This is due to the well known excellent electrocatalytic properties of Pt for the ORR [6].

Carbon cathodes used in this work exhibit a volumetric power generation of 8.1 W m^{-3}, which is lower than the volumetric power production reached in some other studies [34,37], where power densities of 15 and 65 W m^{-3} were obtained using graphite felt biocathodes. Power densities of 24.7 and 68.4 W m^{-3} were achieved with biocathodes based on graphite fiber brushes [35,39]. Differences in power densities can be attributed to the operation conditions, MFC design and cathode surface area. A higher cathode area will increase power generation [40], while cathode active thickness in our tests did not exceed 0.1 mm with a surface area of 50 cm^2. However, even lower power outputs were observed in some other studies with a large surface area, between 2.6 and 4.4 W m^{-3} [8,33,41].

Our experimental results in this work also show that MFCs based on Mn_2O_3 exhibit a power density of 31.7 W m^{-3} (j_{max} of 0.55 mA cm^{-2}) (Fig. 5). This is the highest performance of a MFC based on manganese cathodes until now. Few studies have previously been performed with MnO_2 cathodes [9,10] that have indicated power densities of 3.8 W m^{-3} (j_{max} of 0.01 mA cm^{-2}) [10] and 1.3 W m^{-3} (j_{max} of 0.11 mA cm^{-2}) [9]. In our study, an open circuit potential (OCP) of 635 mV was obtained whereas OCPs of 565 [10] and 715 mV [9] were obtained with MnO_2 cathodes. A systematic comparison of these results is difficult because of the differences in the oxide composition and loading (0.2 mg cm^{-2} in our study vs 0.8 mg cm^{-2} in [9] and 8 mg cm^{-2} in [10]). Even with this significant difference in oxide loading, our catalyst, which has the lowest oxide loading, exhibits the highest power density. These differences in performance might also be attributed to the difference in the electrolyte composition, the contamination of the electrode surface by the biofilm composition and the MFC design. In particular, such improvements in MFC design, as the absence of a PEM, the use of air-breezing cathodes, minimal distance between the electrodes might decrease MFC internal resistance and lead to a higher power density.

The results we obtained for the first time with Fe_2O_3 based cathode indicated that their performance in an MFC is less than those of the Mn_2O_3 based cathode, but more active than the carbon cathode (Table 1 and Fig. 5).

Replacement of air with pure oxygen in the cathode compartment might have several effects on MFC performance as high oxygen levels could affect both cathode and anode performance. Because of O_2 diffusion to the anode, the use of pure O_2 could inhibit anaerobic electricigenic microorganisms and provide an alternative electron acceptor thus reducing the current and decreasing MFC efficiency. On the contrary, the presence of the oxygen at the cathode should improve the ORR. In particular, it should increase the cathode OCP, and contribute to decreasing activation loss and/or improve ORR at reactive sites because of increased oxygen availability [6,35]. This explains the results obtained during the oxygen tests with C, Fe_2O_3 and Mn_2O_3 materials using EIS and polarization tests (Table 1) and COD removal and CE (Table 3). The concentration of the fuel in the cell depends, of course, on its operating conditions.

Table 3 summarizes the COD (chemical oxygen demand) removal and CE (current efficiency). When the cell is operating with the cathodes like Pt or Mn_2O_3 leading to a high COD removal, the concentration of the fuel (acetate of the electrolyte) in the cell will be small whereas it will be high when the cathodes like C with low COD removal is used. In all the cases studied in this work, the initial fuel loading or organic load rate (OLR) was the same at $4\,g\,L^{-1}\,d^{-1}$. This is the common loading used in studies of bio-reactors.

The polarisations tests shown in this work were achieved at a sweeping rate of $0.5\,mV\,s^{-1}$ for a total period of test of 30 min. But other tests performed at low sweeping rates using a low external resistance have shown similar behavior when the tests are done during 1.5 h with a potentiostat or during 3.5 h manually. We did not see significant differences in curves behavior for the measurements done with the same electrochemical parameters evaluated for a given method of polarisation and the different scanning rates and times.

Although Pt cathodes have demonstrated the highest catalytic activity for ORR, the COD removal and the CE are similar if oxygen or air is used as the oxidant (Table 3). This constant performance can be explained by the availability of the electrons coming to the cathode from the anode. In the case of a classical hydrogen/oxygen PEM fuel cell, the Pt oxygen cathode is relatively efficient for the ORR because the hydrogen oxidation is very fast at the anode, which provides sufficient electrons to the cathode for the ORR. The rate of the ORR is 3–4 orders of magnitude smaller than those of the anode reaction. Accordingly, the cathodic reaction limits the overall performance of the H_2/O_2 PEM cell. On the contrary, in the MFC, when the anodic reaction is limited by the biofilm performance, less electrons are produced by the anode. This makes the cathode activity higher than the anode performance. This effect is illustrated in Fig. 6C where the anode potential decreases abruptly under cathodic O_2 atmosphere at a higher current density (maximal produced current) because less electrons are produced at the anode in comparison to the high number of electrons which could be consumed at the cathode for the pure oxygen reduction. This behavior is not observed when the cathode is exposed to air because in this case the ORR performs less when air is used instead of pure oxygen. This statement is supported by the evaluated anodic overpotentials, where an anodic overpotential of 150 mV is observed when a Pt-based MFC working on oxygen in the cathodic compartment, while anodic overpotentials are between 80 and 100 mV for the three other materials. This is as well supported by the EIS and polarization measurements (Table 1), which indicate that a low cathode resistance and high internal resistance are obtained. Thus both cathode and anode activity could be rate limiting in a MFC, but limited anode activity is assumed to be the reason for Pt cathode limitation under O_2.

The results presented above show that the Mn_2O_3 based cathodes might be of interest for developing MFCs with an inexpensive non-noble cathode catalyst. It should be emphasized that in this study Mn_2O_3 cathodes were not optimized and their performance might be further improved. In particular, the activation losses could be decreased by increasing the catalyst loading to values similar to those used in previous studies performed with Mn-oxide based cathodes for MFC applications [9,26]. Another possibility is the modification of the crystalline structure that may enhance its catalytic activity for the ORR [28].

4. Conclusion

Four different cathode materials, C, Fe_2O_3 and Mn_2O_3 and Pt have been tested in this work in order to evaluate their behavior and suitability as ORR catalysts in MFCs. Based on the results obtained in this work, the ORR activity in a classical electrochemical cell with the C, Fe_2O_3 and Mn_2O_3 based cathodes is higher than the ORR activity with the same materials in a MFC. Despite the observation of biofilm formation on the cathode surface, biocathodic activity has not been proven, at least for the duration of the tests in this study (1–2 months). Therefore, it was concluded that biocathodes might exhibit significantly lower ORR activity in MFCs and high-efficiency MFCs might rely on metal catalysts for ORR. Nevertheless, the good performance of the manganese oxides cathode obtained in this work and elsewhere [9,10,42] for the ORR in MFCs is an indication that inexpensive non-noble cathode catalysts could be successfully developed.

Acknowledgements

Funding for this study was provided by NSERC and NRC, Canada (NRC publication number: 53387). The authors would like to thank Monica Nelea and Manon Leduc for their technical analyses as well as Huimin Tian for her experimental assistance.

References

[1] B.E. Logan, B. Hamelers, R. Rozendal, U. Schroder, J. Keller, S. Freguia, P. Aelterman, W. Verstraete, K. Rabaey, Environmental Science and Technology 40 (2006) 5181.
[2] D.R. Lovley, Current Opinion in Biotechnology 19 (2008) 564.
[3] P. Clauwaert, P. Aelterman, T. Pham, L. De Schamphelaire, M. Carballa, K. Rabaey, W. Verstraete, Applied Microbiology and Biotechnology 79 (2008) 901.
[4] F. Harnisch, S. Wirth, U. Schröder, Electrochemistry Communications 11 (2009) 2253.
[5] J. Niessen, U. Schröder, M. Rosenbaum, F. Scholz, Electrochemistry Communications 6 (2004) 5.
[6] H. Rismani-Yazdi, S.M. Carver, A.D. Christy, O.H. Tuovinen, Journal of Power Sources 180 (2008) 683.
[7] F. Zhao, F. Harnisch, U. Schroder, F. Scholz, P. Bogdanoff, I. Herrmann, Environmental Science & Technology 40 (2006) 5193.
[8] H. Tran, J.-H. Ryu, Y.-H. Jia, S.-J. Oh, J.-Y. Choi, D.-H. Park, Water Science & Technology 61 (2010) 1819.
[9] I. Roche, K. Katuri, K. Scott, Journal of Applied Electrochemistry 40 (2010) 13.
[10] L. Zhang, C. Liu, L. Zhuang, W. Li, S. Zhou, J. Zhang, Biosensors and Bioelectronics 24 (2009) 2825.
[11] Y. Yuan, S. Zhou, L. Zhuang, Journal of Power Sources 195 (2010) 3490.
[12] F. Zhao, F. Harnisch, U. Schröder, F. Scholz, P. Bogdanoff, I. Herrmann, Electrochemistry Communications 1405 (2005) 1405.
[13] E. HaoYu, S. Cheng, K. Scott, B. Logan, Journal of Power Sources 171 (2007) 275.
[14] D.H. Park, J.G. Zeikus, Biotechnology and Bioengineering 81 (2003) 348.
[15] N. Duteanu, B. Erable, S.M. Senthil Kumar, M.M. Ghangrekar, K. Scott, Bioresource Technology 101 (2010) 5250.
[16] B. Erable, N. Duteanu, S.M.S. Kumar, Y. Feng, M.M. Ghangrekar, K. Scott, Electrochemistry Communications 11 (2009) 1547.
[17] F. Zhang, S. Cheng, D. Pant, G.V. Bogaert, B.E. Logan, Electrochemistry Communications 11 (2009) 2177.
[18] O. Lefebvre, A. Al-Mamun, W.K. Ooi, Z. Tang, D.H.C. Chua, H.Y. Ng, Water Science & Technology 57 (2008) 2031.
[19] P. Clauwaert, K. Rabaey, P. Aelterman, L. De Schamphelaire, T.H. Pham, P. Boeckx, N. Boon, W. Verstraete, Environmental Science & Technology 41 (2007) 3354.
[20] H.L. Ehrlich, Chemical Geology 132 (1996) 5.

[21] M. Tandukar, S.J. Huber, T. Onodera, S.G. Pavlostathis, Environmental Science & Technology 43 (2009) 8159.
[22] A. Cournet, M.-L. Délia, A. Bergel, C. Roques, M. Bergé, Electrochemistry Communications 12 (2010) 505.
[23] Z. He, L. Angenent, Electroanalysis 18 (2006) 2009.
[24] A.F. Rosenbaum, M. Villano, L.T. Angenent, Bioresource Technology 102 (2010) 324.
[25] B. Erable, I. Vandecandelaere, M. Faimali, M.-L. Delia, L. Etcheverry, P. Vandamme, A. Bergel, Bioelectrochemistry 78 (2010) 51.
[26] M.L. Calegaro, F.H.B. Lima, E.A. Ticianelli, Journal of Power Sources 158 (2006) 735.
[27] J.E. Huheey, A. Keiter, R.L. Keiter, Inorganic Chemistry: Principles of Structure and Reactivity, fourth ed., Harper & Row, New York, 1993, pp. 964.
[28] L. Mao, D. Zhang, T. Sotomura, K. Nakatsu, N. Koshiba, T. Ohsaka, Electrochimica Acta 48 (2003) 1015.
[29] E. Martin, O. Savadogo, S.R. Guiot, B. Tartakovsky, Biochemical Engineering Journal 51 (2010) 132.
[30] E. Barsoukov, J.R. Macdonald, Impedance Spectroscopy – Theory, Experiment, and Applications, John Wiley & Sons, Inc., Hoboken, NJ, 2005, pp. 595.
[31] A. Bergel, D. Féron, A. Mollica, Electrochemistry Communications 7 (2005) 900.
[32] S.E. Oh, J.R. Kim, J.H. Joo, B.E. Logan, Water Science and Technology 60 (2009) 7.
[33] G.-W. Chen, J.-H. Cha, S.-J. Choi, T.-H. Lee, C.-W. Kim, Korean Journal of Chemical Engineering 27 (2010) 828.
[34] K. Rabaey, S.T. Read, P. Clauwaert, S. Freguia, P.L. Bond, L.L. Blackall, J. Keller, ISME Journal 2 (2008) 519.
[35] J.-N. Zhang, Q.-L. Zhao, P. Aelterman, S.-L. You, J.-Q. Jiang, Biotechnology letters 30 (2008) 1771.
[36] B.E. Logan, Microbial Fuel Cells, John Wiley & Sons, Inc., Hoboken, NJ, 2008, pp. 200.
[37] P. Clauwaert, D. van der Ha, N. Boon, K. Verbeken, M. Verhaege, K. Rabaey, W. Verstraete, Environmental Science & Technology 41 (2007) 7564.
[38] S. Yang, B. Jia, H. Liu, Bioresource Technology 100 (2009) 1197.
[39] S.J. You, N.Q. Ren, Q.L. Zhao, J.Y. Wang, F.L. Yang, Fuel Cells 9 (2009) 588.
[40] S.E. Oh, B. Min, B.E. Logan, Environmental Science & Technology 38 (2004) 4900.
[41] P. Liang, M. Fan, X. Cao, X. Huang, Journal of Chemical Technology & Biotechnology 84 (2009) 794.
[42] I. Roche, K. Scott, Journal of Applied Electrochemistry 39 (2009) 197.